Evaluation of Horizon of Viability Optimization Engine for Sustained Power to Critical Infrastructure

Preprint

Vivek Khatana,[1] Soham Chakraborty,[1] Govind Saraswat,[2] Blake Lundstrom,[3] and Murti V. Salapaka[1]

1 University of Minnesota
2 National Renewable Energy Laboratory
3 Enphase Energy

Presented at the IEEE Power and Energy Conference at Illinois (PECI)
Champaign, Illinois
March 10–11, 2022

NREL is a national laboratory of the U.S. Department of Energy
Office of Energy Efficiency & Renewable Energy
Operated by the Alliance for Sustainable Energy, LLC

This report is available at no cost from the National Renewable Energy Laboratory (NREL) at www.nrel.gov/publications.

Contract No. DE-AC36-08GO28308

Conference Paper
NREL/CP-5D00-81800
April 2022

Evaluation of Horizon of Viability Optimization Engine for Sustained Power to Critical Infrastructure

Preprint

Vivek Khatana,[1] Soham Chakraborty,[1] Govind Saraswat,[2] Blake Lundstrom,[3] and Murti V. Salapaka[1]

1 University of Minnesota
2 National Renewable Energy Laboratory
3 Enphase Energy

Suggested Citation
Khatana, Vivek, Soham Chakraborty, Govind Saraswat, Blake Lundstrom, and Murti V. Salapaka. 2022. *Evaluation of Horizon of Viability Optimization Engine for Sustained Power to Critical Infrastructure: Preprint*. Golden, CO: National Renewable Energy Laboratory. NREL/CP-5D00-81800. https://www.nrel.gov/docs/fy22osti/81800.pdf.

© 2022 IEEE. Personal use of this material is permitted. Permission from IEEE must be obtained for all other uses, in any current or future media, including reprinting/republishing this material for advertising or promotional purposes, creating new collective works, for resale or redistribution to servers or lists, or reuse of any copyrighted component of this work in other works.

NREL is a national laboratory of the U.S. Department of Energy
Office of Energy Efficiency & Renewable Energy
Operated by the Alliance for Sustainable Energy, LLC

This report is available at no cost from the National Renewable Energy Laboratory (NREL) at www.nrel.gov/publications.

Contract No. DE-AC36-08GO28308

Conference Paper
NREL/CP-5D00-81800
April 2022

National Renewable Energy Laboratory
15013 Denver West Parkway
Golden, CO 80401
303-275-3000 • www.nrel.gov

NOTICE

This work was authored in part by the National Renewable Energy Laboratory, operated by Alliance for Sustainable Energy, LLC, for the U.S. Department of Energy (DOE) under Contract No. DE-AC36-08GO28308. Funding provided by Advanced Research Projects Agency-Energy (ARPA-E) through the project titled “Rapidly Viable Sustained Grid” via grant no. DE-AR0001016. The views expressed herein do not necessarily represent the views of the DOE or the U.S. Government.

This report is available at no cost from the National Renewable Energy Laboratory (NREL) at www.nrel.gov/publications.

U.S. Department of Energy (DOE) reports produced after 1991 and a growing number of pre-1991 documents are available free via www.OSTI.gov.

Cover Photos by Dennis Schroeder: (clockwise, left to right) NREL 51934, NREL 45897, NREL 42160, NREL 45891, NREL 48097, NREL 46526.

NREL prints on paper that contains recycled content.

Evaluation of Horizon of Viability Optimization Engine for Sustained Power to Critical Infrastructure

Vivek Khatana*,[1], Soham Chakraborty*,[2], Govind Saraswat**,[3], Blake Lundstrom***,[4], and Murti V. Salapaka*,[5]
*Department of Electrical and Computer Engineering, University of Minnesota, USA
**Power Systems Engineering Center, National Renewable Energy Laboratory, Golden, CO 80401, USA
***Enphase Energy, Austin, TX 78758, USA
{[1]khata010, [2]chakr138, [5]murtis}@umn.edu, [3]govind.saraswat@nrel.gov, [4]blakelundstrom@gmail.com

***Abstract*—In the aftermath of increasingly frequent catastrophic events, a typical scenario is critical infrastructure (CI) units being supported by available backup sources with a weak power grid that can be intermittent or absent. Such a scenario is significantly challenging in the sense of providing reliable supply of power to CI units. In this article, an intelligent optimization scheme, termed a horizon of viability (HoV) engine, is developed to guarantee the viability of a sustained, reliable supply of power to the CI units over a time horizon. The proposed HoV engine generates a cost-optimal portfolio of the locally available generation sources and the loads over a time horizon using a mixed-integer convex programming problem. A controller-hardware-in-the-loop (CHIL) platform is developed to evaluate the control performance of the HoV engine. The experimental results corroborate the efficacy in maintaining the viability of the CI units after a grid interruption event. Further, the proposed HoV optimization scheme performs better than existing net-load management schemes in the literature.**

***Index Terms*—Disaster resiliency, generation scheduling, load management, microgrid, mixed-integer programming.**

I. Introduction

The rapid recovery of power flow, possibly after a blackout, is a crucial need arising in scenarios that are increasingly frequent [1]–[3]. The disruption of power to critical infrastructure (CI) units-such as hospitals, medical centers, data centers, etc.-often results in a debilitating impact on physical and economic security, public health and safety. Solutions for the sustained viability of power to CI units in a microgrid, while the grid is being restored, are urgently needed to keep CI units online. Increasingly, the *sustenance* of reliable power requires assistive services to the CI units for long periods of time. Accredited standards like IEEE Std 2030.7 recommend a "dispatch rule"-based optimal energy management system due to its simplicity and low cost in implementation in a microgrid [4]; however, it is primarily concerned with the grid-tie mode of microgrid operation for energy management. Even though the need for energy management during islanded mode is urgent, there has been only sparse effort toward a strategy for ensuring the sustained viability of power to the CI units in a microgrid in the aftermath of the increasingly frequent catastrophic events.

There are some works on the "rule-based" optimal dispatch control of energy resources for microgrids [5]–[9]. In [5], [6], an energy management control scheme with the energy storage system used for power smoothing and state-of-charge (SOC) controlling is proposed for a microgrid with a fixed load; however, critical and deferrable load management of the microgrid, which is crucial when loads are prioritized based on criticality in the system, is not included in the energy management scheme. The works [7]–[9] use a conventional battery cycle-charging strategy which has the disadvantage of shortening battery lifetime through frequent and deep discharges. Moreover, these schemes are primarily focused on generation resource allocation against a fixed and non-vulnerable load in a microgrid. A variety of works in the literature have dealt with the scheduling of deferrable loads in microgrids [10]–[16]. The works [10]–[13] model the deferrable loads as tasks having fixed start and end times with a given energy requirement. This type of deferrable load modeling is not best suited in a constrained scenario when the total generation is less than the total critical and deferrable load demands. In particular, due to the strict start and end times of the deferrable loads, there is less flexibility to switch off certain loads to maintain the supply and demand power balance at all times of operation. This may lead to no load and generation dispatch, reducing the overall quality of service to the critical and deferrable loads in the CI unit. The works [14]–[16] proposed coordinated cost optimal dispatch strategies for deferrable loads. [14] solves a binary programming problem to find a deferrable load action to take for every given frequency deviation with hourly updates. [16] uses dynamic programming approach to find the deferrable load switch-on-off actions for fast frequency response to support the grid. The articles [10]–[16] do not consider optimal scheduling of the available generation sources. The reference [17] compares eight optimization-based coordination frameworks present in the literature that deals only with load scheduling. The reference [18] developed distributed approach

The authors acknowledge the Advanced Research Projects Agency-Energy (ARPA-E) for supporting this research through the project titled "Rapidly Viable Sustained Grid" via grant no. DE-AR0001016. This work was authored in part by the National Renewable Energy Laboratory, managed and operated by Alliance for Sustainable Energy, LLC, for the U.S. Department of Energy (DOE) under Contract No. DE-AC36-08GO28308. The views expressed in the article do not necessarily represent the views of the DOE or the U.S. Government. The U.S. Government retains and the publisher, by accepting the article for publication, acknowledges that the U.S. Government retains a nonexclusive, paid-up, irrevocable, worldwide license to publish or reproduce the published form of this work, or allow others to do so, for U.S. Government purposes.

This report is available at no cost from the National Renewable Energy Laboratory at www.nrel.gov/publications.

for coordinating load aggregators that integrates with automatic generation control for secondary frequency response. The authors in [19] proposed a centralized solution for load control with pre-coordinated day-ahead estimated parameters. The article [20] demonstrated similar combined load control capabilities wherein resources grid tied resources run with static droop characteristics and a direct load frequency control approach is utilized to generate load actions. The authors in [21] proposed a scheme for the dispatch of distributed energy resources, including renewable generation and storage reserves; however, similar to [10]–[13], [21] considers the deferrable loads as tasks. Further, grid support to provide bulk power to support the critical load requirements is assumed. Such a reliable source of power delivery is not present in the case of a catastrophic event, which is the main focus of this work. Unlike [10]–[16], [18]–[21], where the presence of a grid is required and the power available from the grid is used to dispatch loads under normal operating conditions, the scheme developed in this article emphasizes keeping the CI unit online with the objective of maximizing the time horizon of power viability by optimally scheduling the locally available generation resources and deferrable loads at and surrounding the CI unit in the event of a disaster. The contributions of this article are as follows:

1) We develop a net-load (generation and load) dispatch scheme, termed horizon of viability (HoV) engine, to optimally schedule the locally available generation sources and the deferrable loads to provide guaranteed viability of power to the CI unit over a time horizon in the event of a catastrophe leading to the disruption of power from the main grid.

2) We evaluate the HoV engine using controller-hardware-in-the-loop (CHIL) based real-time simulation. These laboratory-based testing results establish the efficacy of the proposed HoV engine in guaranteeing the power viability to CI units in an islanded scenario.

3) We compare the performance of the proposed HoV engine with an existing net-load management [16] system to demonstrate the advantage of the proposed scheme over the existing algorithms in the literature.

The paper is organized as follows: Section II provides definitions, the problem formulation, and the motivation of the current article. The proposed HoV engine is presented in Section III. We also discuss some heuristics to reduce the run time of the HoV integer programming problem. The performance of the HoV engine is demonstrated in a real-time CHIL experiment in Section IV. We also compare the HoV engine with an existing scheme [16] in the literature. Section V provides the conclusion.

II. Problem Formulation and Motivation

A. Definition, Notations, and Assumptions

In this section, we present definitions and notations that are used in the subsequent development.

Definition 1. *(Critical and Deferrable Load) We call a load a critical load (CL) if it does not have any flexibility associated with its control (on/off) and its power requirement must be met whenever requested during the time of operation. We call a load deferrable load (DL) if the power delivery to the load can be deferred. The j^{th} DL being on/off implies that the power delivered to the j^{th} DL is equal to nonzero/zero power.*

Definition 2. *(State of Charge and State of Energy) The state of charge (SOC) of the j^{th} battery, denoted by s_{b_j}, is the level of charge of an electric battery relative to its capacity. Similarly, the state of energy (SOE) of the j^{th} stand-alone diesel generator, denoted by s_{g_j}, is the amount of energy equivalent fuel remaining relative to its reserve capacity.*

Definition 3. *(Net-Load Resource) A collection of resources including distributed energy resources like battery inverter systems, stand-alone diesel generators, renewable energy sources, and deferrable loads is called a net-load resource.*

B. Problem Formulation

Consider a microgrid with a CI unit electrically connected via power lines with surrounding community building (CB) units. The microgrid, as a whole, contains a collection of net-load resources: n_d number of DLs, n_c number of CLs, n_g number of diesel generators, n_p number of renewable generation sources including solar PV inverters and/or wind generators, etc., n_b number of grid-following (GFL) battery inverter systems; and a slack bus (combining all the grid-forming inverter systems in the microgrid) to maintain stable voltage and frequency in the microgrid. We assume that the renewable generation exhibits significant variability. Let $P^t_{r_j}$ denote the renewable generation power of the j^{th} renewable energy resource at time t. The power delivered by the j^{th} diesel generator and the j^{th} GFL battery inverter at time t are denoted by $P^t_{g_j}$ and $P^t_{b_j}$, respectively. The power delivered by the slack bus at time t is denoted by P^t_s. Unlike the diesel generator, the GFL battery inverters are allowed both, to discharge with a positive power output and/or charge with a negative power set point, depending on the net-load and the respective SOCs. Here, each battery inverter, j, is characterized by the maximum available energy capacity, E_{b_j}, and the maximum discharging, W_{b_j}, and charging, $-W_{b_j}$, power transfer rates. The maximum capacity of the j^{th} diesel generator and the slack bus are denoted by W_{g_j} and W_s, respectively. The maximum available energy in the diesel generator, j, at the start of the time, t_0, of the horizon is denoted by E_{g_j}.

C. Motivation and Objective

Consider a grid interruption event when a large portion of grid power is disrupted and the microgrid containing the CI unit is working in an islanded mode while being supported by its own available backup sources and surrounding CB units. The objective of the microgrid is to sustain the CLs in the microgrid and DLs in the CI unit by utilizing *only* the available backup generation-such as the stand-alone diesel generators, battery inverter systems, and the locally available uncertain renewable power generation-until the grid support comes back. A trivial solution for the microgrid is to shut down all the DLs

This report is available at no cost from the National Renewable Energy Laboratory at www.nrel.gov/publications.

of the CB units and utilize the available generation to only support the CI unit and the CLs of the CB units; however, this might lead to a reduced quality of service in the microgrid due to *no* DLs in the CB units being served, leading to discomfort for the consumers in the microgrid. Hence, there is a need to devise an optimal scheduling policy for the net-load resources in the microgrid. Toward this objective, we propose an optimization algorithm, called the HoV engine, which determines a portfolio of generation and load to guarantee the viability of all the CLs in the microgrid while maximizing the level of service of the DLs in the microgrid over a given time horizon.

III. HoV Engine Optimization Problem

Here, a convex optimization problem is solved at each discrete time instant, t_0, to determine the net-load scheduling decisions at some future time instant, $t_0 + t$, where $t \in \{1, 2, \ldots, T\}$, with T being the horizon length. The dispatch decisions are based on renewable generation forecasts, predicted profiles of the DLs, CLs in the microgrid, and information about the latest SOC and SOE of the GFL battery inverters and diesel generators, respectively. This process is repeated at the subsequent time instants with updated sets of measurements. Denote by $x^t := [x_1^t, x_2^t, \ldots x_{n_d}^t] \in \{0,1\}^{n_d}, P_g^t = [P_{g_1}^t, P_{g_2}^t, \ldots P_{g_{n_g}}^t] \in \mathbb{R}^{n_g}, P_b^t = [P_{b_1}^t, P_{b_2}^t, \ldots P_{b_{n_b}}^t] \in \mathbb{R}^{n_b}$, and $P_s^t \in \mathbb{R}$, $\mathbb{T}_{t_0} := \{t_0, \ldots, T + t_0 - 1\}$. The HoV engine optimization problem at any time, t_0, has the following components:

A. Optimization Variables

a) $\mathbf{x} = [x^t, t \in \mathbb{T}_{t_0}] \in \{0,1\}^{n_d \times T}$, where, x^t denotes the ON/OFF decisions of the DLs at time t
b) $\mathbf{P}_b = [P_b^t, t \in \mathbb{T}_{t_0}] \in \mathbb{R}^{n_b \times T}$, where P_b^t is the power set points of the GFL battery inverters at time t
c) $\mathbf{P}_g = [P_g^t, t \in \mathbb{T}_{t_0}] \in \mathbb{R}^{n_g \times T}$, where P_g^t is the power set points of the diesel generators at time t
d) $\mathbf{P}_s = [P_s^t, t \in \mathbb{T}_{t_0}] \in \mathbb{R}^T$, where P_s^t is the slack bus power required to maintain the load and generation power balance at time t.

Let $\pi := [\mathbf{x}, \mathbf{P}_b, \mathbf{P}_g, \mathbf{P}_s]$ denote a policy of net-load dispatch decisions over the horizon $[t_0, t_0 + T]$.

B. Real Time Measurements

a) $s_b^{t_0} = [s_{b_j}^{t_0}, j = 1, \ldots, n_b] \in [0,1]^{n_b}$, where, $s_{b_j}^{t_0}$ denotes the SOC of the GFL battery j at time t_0
b) $s_g^{t_0} = [s_{g_j}^{t_0}, j = 1, \ldots, n_g] \in [0,1]^{n_g}$, where, $s_{g_j}^{t_0}$ denotes the SOE of the diesel generator j at time t_0.

C. Predicted Variables

a) $\hat{P}_L^t = [\hat{P}_{L_j}^t, j = 1, \ldots, n_d, t \in \mathbb{T}_{t_0}] \in \mathbb{R}^{n_d \times T}$, where $\hat{P}_{L_j}^t$ is the predicted load profile of the DL j at time t
b) $\hat{P}_c^t = [\hat{P}_{c_j}^t, j = 1, \ldots, n_c, t \in \mathbb{T}_{t_0}] \in \mathbb{R}^{n_c \times T}$, where $\hat{P}_{c_j}^t$ is the predicted load profile of the CL j at time t
c) $\hat{P}_r^t = [\hat{P}_{r_j}^t, j = 1, \ldots, n_p, t \in \mathbb{T}_{t_0}] \in \mathbb{R}^{n_p \times T}$, where $\hat{P}_{r_j}^t$ is the predicted power output of the j^{th} renewable energy source at time t.

D. Cost Function

$$\mathcal{C}(\mathbf{x}, \mathbf{P}_g, \mathbf{P}_b, s_b, s_g) = \sum_{t=t_0}^{T+t_0-1} \Big[\sum_{j=1}^{n_b} c_{b_j}(s_{b_j}^{t_0}, P_{b_j}^t) - \sum_{j=1}^{n_g} c_{g_j}(\eta_{g_j}(P_{g_j}^t)) + \sum_{j=1}^{n_d} c_{\ell_j}(1 - x_j^t)\hat{P}_{L_j}^t \Big].$$

The first term captures the cost of dispatching the GFL battery inverters. $c_{b_j}(.)$ is a convex function and ensures a cost-optimal charging/discharging dispatch of the GFL battery inverters over the horizon $[t_0, t_0 + T]$ based on the SOC of the GFL batteries. The second term captures the cost of dispatch for the diesel generators. The function $c_{g_j}(.)$ is a concave function of the arguments $\mathbf{P}_g^{t_0}$ and $s_g^{t_0}$. The function c_{g_j} enforces that the diesel generators are dispatched over the horizon $[t_0, t_0+T]$ at a higher efficiency set-point $\eta_{g_j}(P_{g_j}^t)$ for maximum utilization of the available stand-alone diesel generator storage. The last term generates an optimal portfolio of loads to be switched on (a DL j is *on* at time t if and only if $x_j^t = 1$) during the horizon $[t_0, t_0 + T]$ based on the load switched-off costs c_{ℓ_j}. The costs, c_{ℓ_j}, are decided based on the relative priorities of the DLs and the effect of switching the particular load off on the overall discomfort for the users in the microgrid. Together, the three terms in the cost function ensure that the CI units remain viable over the horizon. Further, the discomfort due to switching off a lot of DLs in the microgrid is also minimized.

E. Optimization Problem

Let $\tilde{s}_{b_j}^{t_0} := -(1 - s_{b_j}^{t_0})$,

$$\Lambda := \underset{\pi}{\text{minimize}} \quad \mathcal{C}(\mathbf{x}, \mathbf{P}_g, \mathbf{P}_b, s_b^{t_0}, s_g^{t_0}), \quad \text{subject to :}$$

$$0 \leq \sum_{t=t_0}^{T+t_0-1} P_{g_j}^t \leq s_{g_j}^{t_0} E_{g_j}, \text{ for } j = 1, \ldots, n_g, \tag{1}$$

$$\tilde{s}_{b_j}^{t_0} E_{b_j} \leq \sum_{t=t_0}^{T+t_0-1} P_{b_j}^t \leq s_{b_j}^{t_0} E_{b_j}, \text{ for } j = 1, \ldots, n_b, \tag{2}$$

$$0 \leq P_{g_j}^t \leq W_{g_j}, \text{ for } j = 1, \ldots, n_g, t \in \mathbb{T}_{t_0}, \tag{3}$$

$$-W_{b_j} \leq P_{b_j}^t \leq W_{b_j}, \text{ for } j = 1, \ldots, n_b, t \in \mathbb{T}_{t_0} \tag{4}$$

$$0 \leq P_s^t \leq W_s, \text{ for } t \in \mathbb{T}_{t_0}, \tag{5}$$

$$\sum_{j=1}^{n_d} x_j^t \hat{P}_{L_j}^t + \sum_{j=1}^{n_c} \hat{P}_{c_j}^t = \sum_{j=1}^{n_g} P_{g_j}^t + \sum_{j=1}^{n_b} P_{b_j}^t + \sum_{j=1}^{n_p} \hat{P}_{r_j}^t + P_s^t, \text{ for } t \in \mathbb{T}_{t_0} \tag{6}$$

$$x_j^t \in \{0,1\}, \text{for } j = 1, \ldots, n_d, \text{ for } t \in \mathbb{T}_{t_0}. \tag{7}$$

F. Constraints

1) Available Energy Over the Horizon: Constraints (1) and (2) limit the maximum and minimum amount of total energy served to the loads during the horizon $[t_0, t_0+T]$ based on the available energy in the stand-alone diesel generators and the GFL inverters at the start of the horizon.

This report is available at no cost from the National Renewable Energy Laboratory at www.nrel.gov/publications.

2) Generation: Constraints (3)-(5) enforce the maximum and minimum capacity limits on the power dispatch of the diesel generators, GFL inverters, and the slack bus.

3) Power Balance: Constraint (6) ensures that the sum of all the power allocations to the critical loads and deferrable loads is equal to the available total generation.

4) Load Selection: Constraint (7) is the binary constraint to decide the deferrable load switch-on-off status.

The solution, π^*, to the optimization problem, Λ, is utilized as the net-load dispatch decision for the microgrid containing the CI unit, with P_g^* and P_b^* being the diesel generator and the battery set points, respectively; P_{slk}^* being the slack battery power to be utilized; and x^* being the load switch-on-off decisions.

G. Heuristics to Improve the Run time of the HoV Optimization Problem

Recall that the HoV optimization problem, Λ, due to the binary constraint (7), used for the load selection, is a mixed integer programming problem, which can be very hard to solve in general [22]. The solution time for the problem, Λ, can be improved by using the following heuristics:

1. The equality constraint (6) can be relaxed by specifying an operating band based on the power mismatch that can be safely tolerated by the slack bus. In particular, the constraint (6) can be equivalently written as a set of two inequality constraints: for $t \in \mathbb{T}_{t_0}$,

$$\underline{\delta}\big[\sum_{j=1}^{n_g} P_{g_j}^t + \sum_{j=1}^{n_b} P_{b_j}^t + \sum_{j=1}^{n_p} \hat{P}_{r_j}^t + P_s^t\big] \leq \sum_{j=1}^{n_d} x_j^t \hat{P}_{L_j}^t + \sum_{j=1}^{n_c} \hat{P}_{c_j}^t \leq \overline{\delta}\big[\sum_{j=1}^{n_g} P_{g_j}^t + \sum_{j=1}^{n_b} P_{b_j}^t + \sum_{j=1}^{n_p} \hat{P}_{r_j}^t + P_s^t\big],$$

where, $\overline{\delta} \in (0,1], \underline{\delta} \in (0, \overline{\delta}]$. The exact values of $\overline{\delta}$ and $\underline{\delta}$ can be chosen based on the application. Note that $\overline{\delta} = \underline{\delta} = 1$ recovers the original constraint (6).

2. Providing a good initial guess of the optimal solution to the optimization solver also improves the run time. A good initial solution for the problem, Λ, can be obtained by finding the optimal set of deferrable loads to be switched on at the starting time instant t_0 and assuming that the same set of deferrable loads remains operational throughout the horizon $[t_0, t_0 + T]$ based on the instantaneous power generation measurements $\{P_{g_j}^{t_0}, P_{b_j}^{t_0}\ \forall j\}$ from the microgrid. In particular, consider the simpler problem,

$$\begin{aligned} \underset{x}{\text{minimize}} \quad & \sum_{j=1}^{n_d} c_{\ell_j}(1 - x_j)\hat{P}_{L_j}^{t_0}, \quad \text{subject to :} \\ & 0 \leq \sum_{j=1}^{n_d} x_j \hat{P}_{L_j}^{t_0} + \sum_{j=1}^{n_c} \hat{P}_{c_j}^{t_0} - \sum_{j=1}^{n_g} P_{g_j}^{t_0} \\ & \qquad - \sum_{j=1}^{n_b} P_{b_j}^{t_0} - \sum_{j=1}^{n_p} \hat{P}_{r_j}^{t_0} \leq W_s, \\ & x_j \in \{0,1\}, \text{ for } j = 1, \ldots, n_d. \end{aligned}$$

The solution $x^t = x$ for $t \in \mathbb{T}_{t_0}$ can be taken as an initial solution to the variable $\mathbf{x}^{t_0}$ the in HoV optimization problem, Λ.

IV. CHIL Demonstration and Results

Fig. 1 shows the three-phase microgrid test system under study that contains 1 CI unit and the surrounding 3 CB units. The ratings of various sources, loads, and line parameters are tabulated in Table I. On top of the power layer, there is a communication layer that enables the transmission of various measurements, from the system to the HoV engine, and various control signals, from the HoV engine to the microgrid. The extensive list of measurements and control signals is shown in the schematic of the CHIL-based real time implementation of the HoV engine with the microgrid in Fig. 2. There are three important components in the demonstration: (i) the microgrid, emulated using the eMEGASIM platform with a simulation step size of 50μs inside the OP5700 RT-simulator (RTS), which is manufactured by OPAL-RT and interfaced with two low-cost Texas Instruments TMS320F28379D, 16/12-bit floating-point 200-MHz Delfino microcontroller boards for controlling two GFM inverters in the CB-1 and CB-2 units; (ii) the HoV optimization engine running on a server workstation, developed using Python 3.7.1 with commercial optimization solver, MOSEK [23] to solve the mixed integer convex programming problem, Λ of Section III-E; and (iii) a Device Control Gateway (DCG), realized using standard User Datagram Protocol (UDP) [24], that interfaces the microgrid and the HoV engine and emulates the communication layer that continuously listens to the measurements sent from the microgrid and dispatch commands from the HoV engine. Realistic load profiles and the solar irradiance profile are fed into the real-time simulator with 1-s resolution. Most of the load profiles are obtained through the metering system by the energy management group of the University of Minnesota, and, the rest are synthetically generated. Real-world solar irradiance data for the study are obtained from the National Renewable Energy Laboratory's solar Measurement and Instrumentation Data Center and the National Solar Radiation

TABLE I
RATINGS OF VARIOUS GENERATION SOURCES, LOADS, AND LINE PARAMETERS OF THE MICROGRID UNDER STUDY

Generation and Load (kW)	**Microgrid Test System**			
	CI Unit	**CB Unit 1**	**CB Unit 2**	**CB Unit 3**
PV	50	100	100	150
GFL Bat-1	100	-	-	-
GFL Bat-2	100	-	-	-
GFM Bat	-	200	250	200
Diesel Gen-1	50	-	-	-
Diesel Gen-2	50	-	-	-
Critical Load	230	100	225	150
Deferrable Load	350	300	275	350

Microgrid Network	**Values**
Transformers	3-ϕ, Y-Y, 1 MVA, 13.8/0.48 kV
Line Parameters	R_{line} = 5 mΩ, L_{line} = 30 μH

This report is available at no cost from the National Renewable Energy Laboratory at www.nrel.gov/publications.

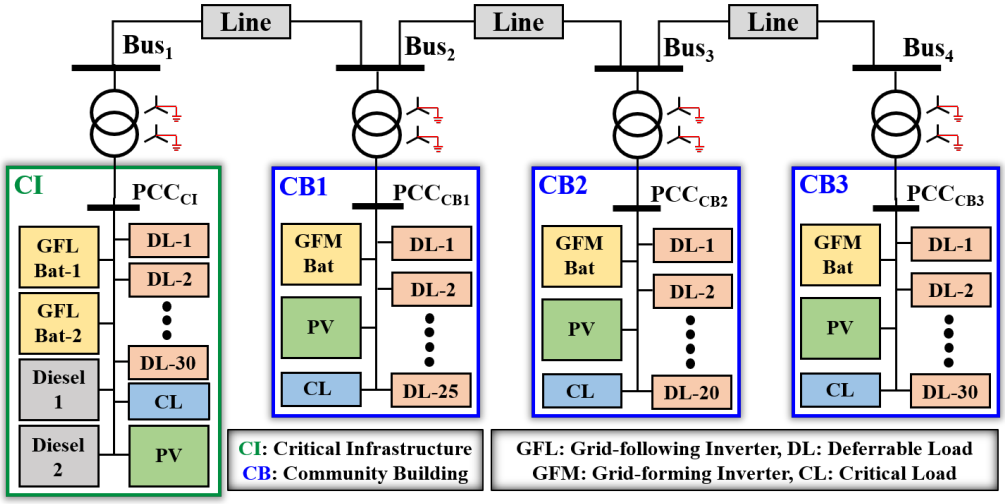

Fig. 1. The microgrid test system contains 1 critical infrastructure (CI) unit and 3 community building (CB) units. The CI unit contains 2 GFL battery inverters, 2 diesel generators, 1 PV inverter system, 1 critical load (CL), and 30 deferrable loads (DLs). Similarly, CB-1, CB-2, and CB-3 contain 1 GFM battery inverter each, 1 PV inverter system each , 1 CL each, and 25, 20, and 30 DLs, respectively.

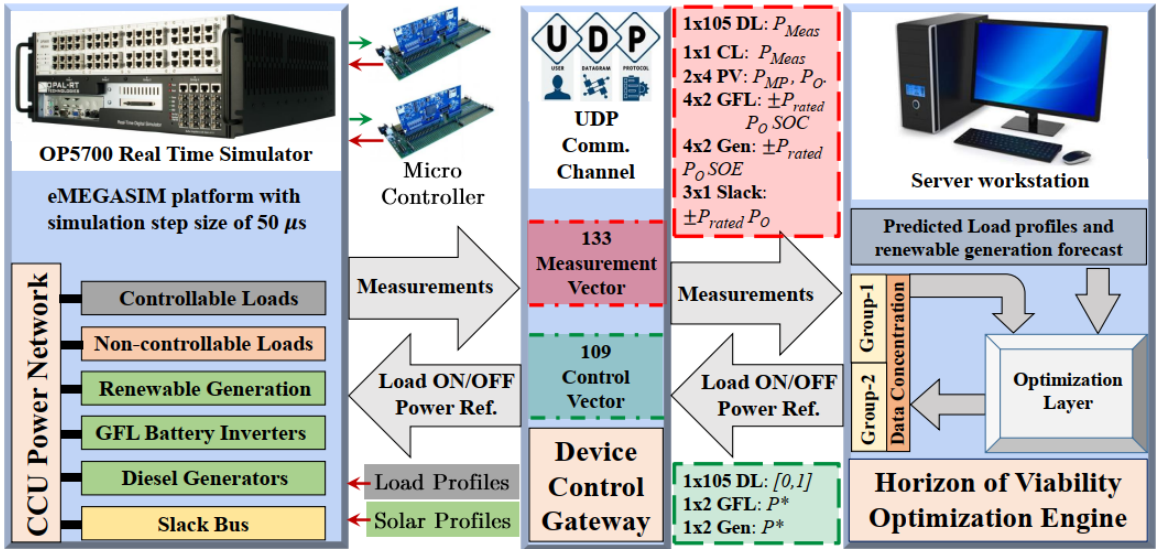

Fig. 2. Schematic of the CHIL-based demonstration of the HoV optimization engine.

Database [25]. A 2-hour experiment is conducted for the validation of the proposed HoV engine. Moreover, to show the efficacy, a comparative study is conducted with the net-load management (NLM) scheme existing in the literature [16].

To evaluate the performance of the developed HoV optimization engine, we define the following metrics:

1) Total Remaining Energy (TRE): The TRE (in kWh) in the local generation sources in the microgrid (i.e, GFL battery inverters and diesel generators in the CI units of the microgrid) at the end of the time horizon $[0, \mathcal{T}]$ is defined as:

$$\text{TRE}(\mathcal{T}) := \sum_{j=1}^{n_g} s_{g_j}^{\mathcal{T}} E_{g_j} + \sum_{j=1}^{n_b} s_{b_j}^{\mathcal{T}} E_{b_j}. \tag{8}$$

2) Cost-Weighted Energy (CWE): The total CWE delivered to all critical and deferrable loads in the microgrid over a time horizon $[0, \mathcal{T}]$ is defined as:

$$\text{CWE}(\mathcal{T}) := \int_0^{\mathcal{T}} \sum_{i=1}^{n_d+n_c} c_{\ell_i} p_{L_i}^t dt, \tag{9}$$

where, $p_{L_i}^t$ is the per-unit power of load i.

The metrics in (8) and (9) capture the trade-off between the guaranteed viability of power for the CI units (higher remaining energy implies the availability of more energy in the generation resources of the CI units) and the level of service of the required CLs and DLs (higher CWE implies that more higher-priority loads are running). For comparison with the existing NLM scheme, we also define the ratios of the CWE

This report is available at no cost from the National Renewable Energy Laboratory at www.nrel.gov/publications.

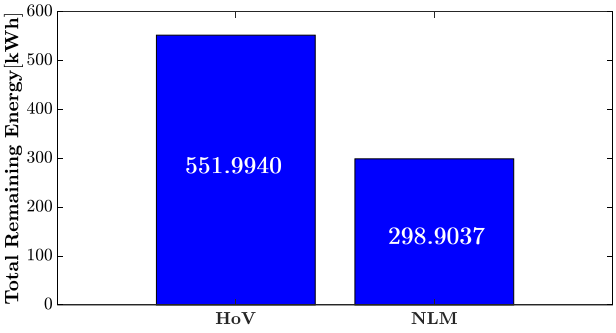

Fig. 3. Total remaining energy (in kWh) after 2 hours of the CHIL experiment of the proposed HoV engine and existing NLM engine on the test system in Fig. 1.

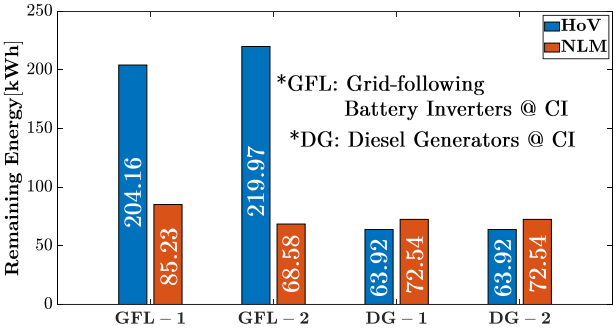

Fig. 4. Remaining energy (in kWh) in each generating resource (2 GFL batteries and 2 diesel generators) in the CI unit after 2 hours of the CHIL experiment of the proposed HoV engine and the existing NLM engine on the test system in Fig. 1.

and TRE metrics for the proposed HoV engine and the existing NLM engine. Specifically, we define the following:

$$\rho_{\text{CWE}}(t) := \frac{\text{CWE}_{\text{HoV}}(t)}{\text{CWE}_{\text{NLM}}(t)}, \tag{10}$$

$$\rho_{\text{TRE}}(t) := \frac{\text{TRE}_{\text{HoV}}(t)}{\text{TRE}_{\text{NLM}}(t)}. \tag{11}$$

Note that $n_g = 2$, $n_b = 2$, $n_d = 105$, $n_c = 1$, and $\mathcal{T} = 2$ hours (7200 s) for the CHIL experiment with the microgrid test system under study, as shown in Fig. 1.

Figs. 3-6 demonstrate the performance of the HoV engine compared to the NLM engine [16] with respect to the TRE and CWE metrics. Fig. 3 provides a comparison based on the total remaining energy. The HoV optimization engine optimally schedules the available generation sources that result in a higher total remaining energy available at the end of 2 hours that can be utilized to serve the critical loads in the CI and CB units at a later time instant. The breakdown of the total energy remaining (among the 2 GFL batteries and 2 diesel generators) is presented in Fig. 4. This shows the advantage of the proposed HoV engine over the existing NLM engine in the sense of extending the horizon of the viable operation of the CI units in a microgrid. Fig. 5 demonstrates that the HoV engine provides more total CWE than the NLM engine over the 2 hour horizon; therefore, the HoV engine provides

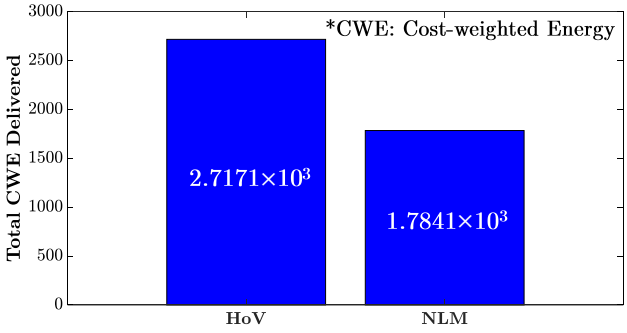

Fig. 5. Total cost-weighted energy after 2 hours of the CHIL experiment of the proposed HoV engine and the existing NLM engine on the test system in Fig. 1.

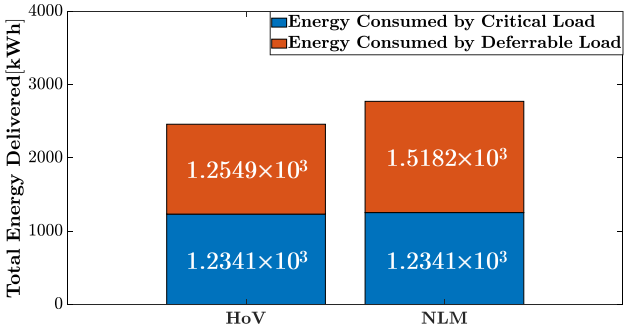

Fig. 6. Total energy delivered after 2 hours of the CHIL experiment of the proposed HoV engine and the existing NLM engine on the test system in Fig. 1.

power to more high-priority deferrable loads during the time duration of the experiment. Fig. 6 shows that the total energy (kWh) delivered to the deferrable loads is more in the NLM dispatch; however the HoV engine better respects the load priorities than the NLM engine, as demonstrated by the benefit in terms of the CWE in Fig. 5. This shows the benefit of the HoV engine in supplying power to the higher-prioritized loads in a resource-constrained scenario.

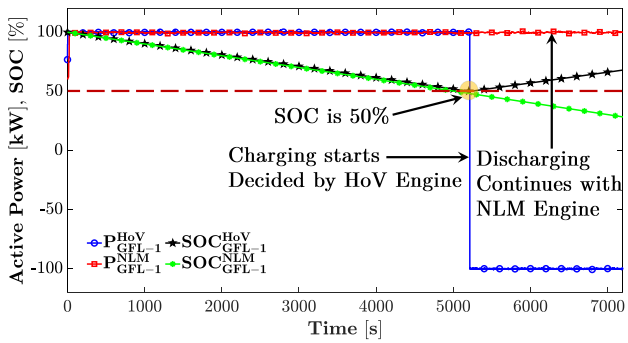

Fig. 7. Active power output and SOC of the GFL battery-1 in the CI unit during 2 hours of the CHIL experiment with the proposed HoV engine and the existing NLM engine on the test system in Fig. 1.

The behaviour of the HoV engine during the experiment is presented in Figs. 7 and 8. Although the diesel generators are always operated at a high efficiency set-point near the rated

This report is available at no cost from the National Renewable Energy Laboratory at www.nrel.gov/publications.

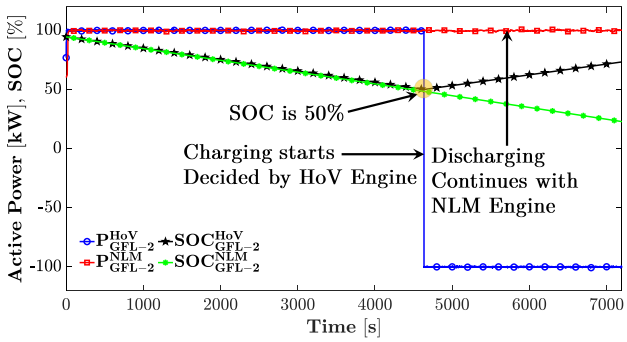

Fig. 8. Active power output and SOC of the GFL battery-2 in the CI unit during 2 hours of the CHIL experiment with the proposed HoV engine and the existing NLM engine on the test system in Fig. 1.

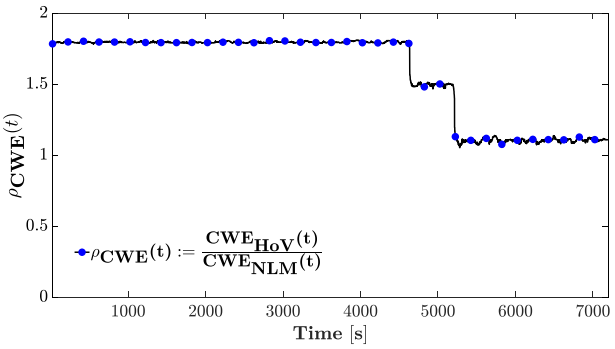

Fig. 9. Ratio of the CWE metric value resulting from HoV engine and NLM engine during 2 hours of CHIL experiment on the test system of Fig. 1.

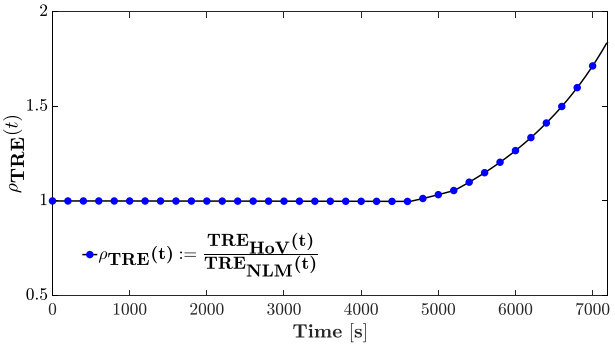

Fig. 10. Ratio of the TRE metric value resulting from HoV engine and NLM engine during 2 hours of CHIL experiment on the test system of Fig. 1.

capacity, the HoV engine intelligently controls the GFL battery inverters based on the current SOC of the battery sources. It can be observed here that initially both the HoV and the NLM engine are inclined toward running more load in the microgrid, and, as a result, the power set points are at the rated peak for both GFL batteries. Unlike the NLM engine, however, the HoV engine moves to the GFL battery-saving mode by generating charging commands for both GFL batteries after an instance when the SOCs of the GFL batteries fall below 50%. Therefore, initially, the HoV engine is aggressive in terms of maintaining a good quality of service to the load, but it adjusts itself to conserve generation for future times of operation. The NLM engine, on the other hand, does not adjusts itself to address future contingencies of power delivery to the CI units, which is demonstrated by a lower SOC in the GFL batteries (Figs. 7 and 8) and consequently lower total energy remaining in the generation sources (Fig. 3 and Fig. 4). This behavior of the proposed HoV engine and the NLM engine can be further corroborated by referring to Fig. 9 and Fig. 10. These two figures show the run time ratios of the CWE and TRE metrics (ρ_{CWE} and ρ_{TRE}), defined in (10) and (11). It can be observed that the proposed HoV engine is equally conservative in restoring the energy of the GFL batteries in the CI unit but more aggressive in terms of supplying a higher number of prioritized loads in the microgrid compared to the NLM engine (indicated by $\rho_{\text{CWE}} > 1$ and $\rho_{\text{TRE}} \approx 1$). Yet, toward the end of the horizon, the HoV engine is more aggressive in restoring the energy of the GFL batteries in the CI unit but equally aggressive in terms of supplying prioritized loads in the microgrid compared to the NLM engine (indicated by $\rho_{\text{CWE}} \approx 1$ and $\rho_{\text{TRE}} > 1$).

V. Conclusion

In the aftermath of increasingly frequent catastrophic events, a reliable and sustained supply of power to critical infrastructure units in a microgrid is becoming a crucial need. In this article, an intelligent optimization scheme, termed a horizon of viability (HoV) engine, is developed to guarantee the viability of a sustained, reliable supply of power to critical infrastructure units over a time horizon, after a grid failure. The proposed HoV engine generates a cost-optimal portfolio of the locally available generation sources and the loads over a time horizon using a mixed-integer convex programming problem. A CHIL platform is developed to evaluate the control performance of the HoV engine. The experimental results corroborate the efficacy in maintaining the viability of the CI units after a grid interruption event. Further, the proposed HoV optimization scheme performs better than the existing net-load management schemes in the literature.

References

[1] N. Kishore, D. Marqués, A. Mahmud, M. V. Kiang, I. Rodriguez, A. Fuller, P. Ebner, C. Sorensen, F. Racy, J. Lemery *et al.*, "Mortality in puerto rico after hurricane maria," *New England journal of medicine*, vol. 379, no. 2, pp. 162–170, 2018.

[2] R. J. Campbell and S. Lowry, "Weather-related power outages and electric system resiliency." Congressional Research Service, Library of Congress Washington, DC, 2012.

[3] E. institue at UT Austin, "The timeline and events of the february 2021 texas electric grid blackouts," 2021, [November 18, 2021]. [Online]. Available: https://energy.utexas.edu/ercot-blackout-2021

[4] "Ieee standard for the specification of microgrid controllers," *IEEE Std 2030.7-2017*, pp. 1–43, 2018.

[5] C. Sun, G. Joos, S. Q. Ali, J. N. Paquin, C. M. Rangel, F. A. Jajeh, I. Novickij, and F. Bouffard, "Design and real-time implementation of a centralized microgrid control system with rule-based dispatch and seamless transition function," *IEEE Transactions on Industry Applications*, vol. 56, no. 3, pp. 3168–3177, 2020.

[6] S. Manson, B. Nayak, and W. Allen, "Robust microgrid control system for seamless transition between grid-tied and island operating modes," in *44th Annual Western Protective Relay Conference*, 2017.

This report is available at no cost from the National Renewable Energy Laboratory at www.nrel.gov/publications.

[7] A. M. Ameen, J. Pasupuleti, and T. Khatib, "Simplified performance models of photovoltaic/diesel generator/battery system considering typical control strategies," *Energy Conversion and Management*, vol. 99, pp. 313–325, 2015.
[8] B. Zhao, X. Zhang, P. Li, K. Wang, M. Xue, and C. Wang, "Optimal sizing, operating strategy and operational experience of a stand-alone microgrid on dongfushan island," *Applied Energy*, vol. 113, pp. 1656–1666, 2014.
[9] C. Sun, G. Joos, and F. Bouffard, "Adaptive coordination for power and soc limiting control of energy storage in an islanded ac microgrid with impact load," *IEEE Transactions on Power Delivery*, vol. 35, no. 2, pp. 580–591, 2019.
[10] D. Materassi, S. Bolognani, M. Roozbehani, and M. A. Dahleh, "Deferrable loads in an energy market: Coordination under congestion constraints," in *22nd Mediterranean Conference on Control and Automation*. IEEE, 2014, pp. 628–633.
[11] A. Subramanian, M. Garcia, A. Dominguez-Garcia, D. Callaway, K. Poolla, and P. Varaiya, "Real-time scheduling of deferrable electric loads," in *2012 American Control Conference (ACC)*. IEEE, 2012, pp. 3643–3650.
[12] L. Gan, A. Wierman, U. Topcu, N. Chen, and S. H. Low, "Real-time deferrable load control: handling the uncertainties of renewable generation," in *Proceedings of the fourth international conference on Future energy systems*, 2013, pp. 113–124.
[13] S. Haque, D. Materassi, S. Bolognani, M. Roozbehani, and M. A. Dahleh, "An efficient partial-order representation of feasible schedules for online decisions," in *2017 IEEE 56th Annual Conference on Decision and Control (CDC)*. IEEE, 2017, pp. 2641–2646.
[14] R. Bhana and T. J. Overbye, "The commitment of interruptible load to ensure adequate system primary frequency response," *IEEE Transactions on Power Systems*, vol. 31, no. 3, pp. 2055–2063, 2015.
[15] X. Wu, J. He, Y. Xu, J. Lu, N. Lu, and X. Wang, "Hierarchical control of residential hvac units for primary frequency regulation," *IEEE Transactions on Smart Grid*, vol. 9, no. 4, pp. 3844–3856, 2017.
[16] B. Lundstrom, S. Patel, and M. V. Salapaka, "Distribution feeder-scale fast frequency response via optimal coordination of net-load resources—part i: Solution design," *IEEE Transactions on Smart Grid*, vol. 12, no. 2, pp. 1289–1302, 2021.
[17] A. G. Azar, H. Nazaripouya, B. Khaki, C.-C. Chu, R. Gadh, and R. H. Jacobsen, "A non-cooperative framework for coordinating a neighborhood of distributed prosumers," *IEEE Transactions on Industrial Informatics*, vol. 15, no. 5, pp. 2523–2534, 2018.
[18] J. Hu, J. Cao, J. M. Guerrero, T. Yong, and J. Yu, "Improving frequency stability based on distributed control of multiple load aggregators," *IEEE Transactions on Smart Grid*, vol. 8, no. 4, pp. 1553–1567, 2015.
[19] L. Tang and J. McCalley, "Two-stage load control for severe under-frequency conditions," *IEEE Transactions on Power Systems*, vol. 31, no. 3, pp. 1943–1953, 2015.
[20] A. M. Prostejovsky, M. Marinelli, M. Rezkalla, M. H. Syed, and E. Guillo-Sansano, "Tuningless load frequency control through active engagement of distributed resources," *IEEE Transactions on Power Systems*, vol. 33, no. 3, pp. 2929–2939, 2017.
[21] A. Subramanian, M. J. Garcia, D. S. Callaway, K. Poolla, and P. Varaiya, "Real-time scheduling of distributed resources," *IEEE Transactions on Smart Grid*, vol. 4, no. 4, pp. 2122–2130, 2013.
[22] L. A. Wolsey, *Integer programming*. John Wiley & Sons, 2020.
[23] M. ApS, "The mosek optimization toolbox for matlab manual. version 9.0." 2019. [Online]. Available: http://docs.mosek.com/9.0/toolbox/index.html
[24] "User datagram protocol," 2021, [November 18, 2021]. [Online]. Available: https://en.wikipedia.org/wiki/User_Datagram_Protocol
[25] [Online]. Available: https://www.nrel.gov/gis/data-tools.html

This report is available at no cost from the National Renewable Energy Laboratory at www.nrel.gov/publications.